AGU PUBLICATIONS

JGR

Journal of Geophysical Research: Space Physics

RESEARCH ARTICLE
10.1002/2016JA022751

This article is a companion to *Moro et al.* [2016] doi:10.1002/2016JA022753.

Key Points:
- Radar data collected from 2001 to 2010 are used to infer the *E* region electric fields in the American sector
- *Ey* ranges from 0.21 to 0.35 mV/m in Brazil and from 0.23 to 0.45 mV/m in Peru, under quiet geomagnetic condition
- *Ez* ranges from 7.09 to 8.80 mV/m in Brazil and from 9.00 to 11.18 mV/m in Peru, under quiet geomagnetic condition

Correspondence to:
J. Moro,
juliano.moro@inpe.br;
julianopmoro@gmail.com

Citation:
Moro, J., C. M. Denardini, L. C. A. Resende, S. S. Chen, and N. J. Schuch (2016), Equatorial *E* region electric fields at the dip equator: 1. Variabilities in eastern Brazil and Peru, *J. Geophys. Res. Space Physics*, *121*, 10,220–10,230, doi:10.1002/2016JA022751.

Received 28 MAR 2016
Accepted 20 SEP 2016
Accepted article online 23 SEP 2016
Published online 14 OCT 2016
Corrected 27 OCT 2016

This article was corrected on 27 OCT 2016. See the end of the full text for details.

Equatorial *E* region electric fields at the dip equator: 1. Variabilities in eastern Brazil and Peru

J. Moro[1], C. M. Denardini[2], L. C. A. Resende[2], S. S. Chen[2,3], and N. J. Schuch[1]

[1]Southern Regional Space Research Center (CRS/INPE), Santa Maria, Brazil, [2]National Institute for Space Research (INPE), São José dos Campos, Brazil, [3]Department of Electrical Engineering, University of Taubaté, Taubaté, Brazil

Abstract The equatorial electrojet (EEJ) is an intense eastward ionospheric electric current centered at about 105 km of altitude along the dip equator, set up by the global neutral wind dynamo that generates the eastward zonal (*Ey*) and the daytime vertical (*Ez*) electric fields. The temporal variation of the EEJ is believed to be well understood. However, the longitudinal variability of the *Ey* and *Ez* between 100 and 110 km is still quite scarce. Due to their importance overall phenomenology of the equatorial ionosphere, we investigate the variabilities of the *Ey* and *Ez* inferred from measurements of the Doppler frequency of Type II echoes provided by coherent backscatter radars installed in locations close to the magnetic equator in the eastern Brazil (2.33°S, 44.20°W) and Peru (11.95°S, 76.87°W). This study is based on long-term (609 days for both systems) radar soundings collected from 2001 to 2010. The variabilities of the electric fields are studied in terms of the position of the soundings with respect to the dip equator and the magnetic declination angle. Among the results, *Ey* and *Ez* show longitudinal dependence, being higher in Peru than east Brazil. Under quiet geomagnetic activity, the mean diurnal variations of *Ey* ranged from 0.21 to 0.35 mV/m between 8 and 18 h (LT) in Brazil and from 0.23 mV/m to 0.45 mV/m in Peru, while the mean diurnal variations of the *Ez* ranges from 7.09 to 8.80 mV/m in Brazil and from 9.00 to 11.18 mV/m in Peru.

1. Introduction

The equatorial electrojet (EEJ) is an intense electric current flowing eastward along the geomagnetic dip latitudes driven basically by the eastward zonal (*Ey*) electric field, which is generated in both daytime and nighttime by the *E* region dynamo [*Forbes*, 1981]. The EEJ represents a rather large enhancement of the diurnal variation in the horizontal component of the geomagnetic field and at the vicinity of the dip equator. The cross field of *Ey* and northward geomagnetic field produces an eastward Pedersen current and a downward Hall current. The Hall current is restricted in the lower and upper boundaries of the dynamo region due to the abrupt dropping in the local conductivities, which leads to an upward daytime vertical (*Ez*) electric field. This field drives gradient drift instability that produces Type II irregularities [*Cohen and Bowles*, 1967], which can act as scattering centers for HF and VHF radio waves.

The most systematic experimental studies of the equatorial ionospheric *E* region have been provided by incoherent backscatter radar observations at the Jicamarca Radio Observatory (JRO) in the Peruvian sector [*Woodman*, 1970; *Farley and Balsley*, 1973; *Farley et al.*, 1978; *Farley*, 1985; *Kudeki and Sürücü*, 1991; *Woodman and Chau*, 2002]. Subsequent incoherent backscatter radar observations were notably from Indian and African sectors [*Reddy and Devasia*, 1976; *Crochet*, 1977; *Crochet et al.*, 1979; *Reddy et al.*, 1987; *Patra et al.*, 2005], confirming the existence of the two types of radar echoes and bringing out characteristic of the diurnal, seasonal, and solar cycle variabilities of the EEJ. Most of the equatorial ionospheric electric field (**E**) were obtained from the vertical drift measurements (**v**) through the standard relation $\mathbf{v} = \mathbf{E} \times \mathbf{B}/B^2$, where **B** is the main magnetic field. However, the numbers of incoherent backscatter radars measuring ionospheric drifts for electric fields inference at equatorial stations are very limited due to the complexity of building and operation. Another way to obtain the electric fields, specific in the EEJ region, is through the use of the Doppler frequency from Type II echoes provided by coherent backscatter radars. This technique has been used to make indirect measurements of the *E* region electric field (EEF) in the Peruvian [*Balsley*, 1973; *Woodman*, 1970; *Balsley and Woodman*, 1971; *Hysell and Burcham*, 2000] and Indian [*Reddy et al.*, 1981, 1987; *Viswanathan et al.*, 1987, 1993] sectors. In the Brazilian sector, coherent backscatter radar technique has being employed for sounding the equatorial *E* region since the 2000s. The measurements have provided several information of the EEJ and its plasma irregularities: short-period (~5 min or larger)

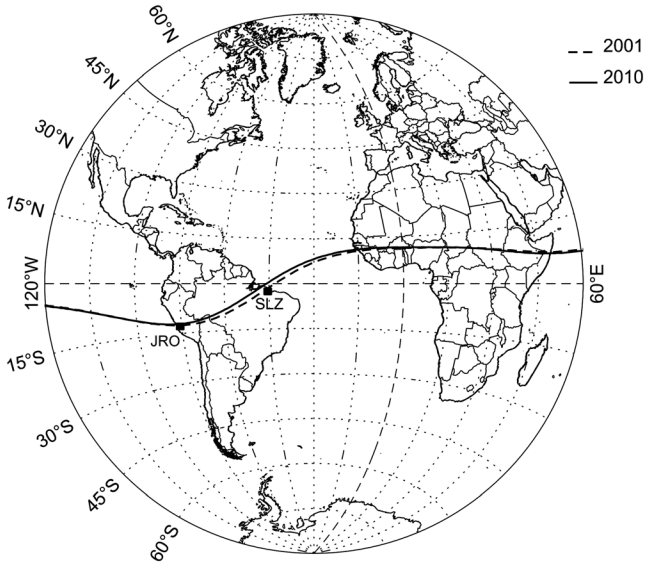

Figure 1. Geographic locations of the São Luís Space Observatory, Brazil (SLZ, 2.33°S, 44.20°W) and the Jicamarca Radio Observatory, Peru (JRO, 11.95°S, 76.87°W). The geomagnetic equator given by the IGRF-11 model is plotted by dashed line in 2001 and in continuous line in 2010.

fluctuations and significant day-to-day variability [*Abdu et al.*, 2002], vertical distributions [*Denardini et al.*, 2003; *de Paula and Hysell*, 2004], variabilities under auroral activity and quiet geomagnetic conditions [*Denardini et al.*, 2004], seasonal characterization [*Denardini et al.*, 2005], transition from daytime to nighttime [*Denardini et al.*, 2006], equatorial counter electrojet events [*Denardini et al.*, 2009], atmosphere-ionosphere coupling process at the *E* region heights due to upward propagating waves from tropospheric source [*Aveiro et al.*, 2009a, 2009b], simultaneous observation of irregularities during late afternoon for quiet and geomagnetic disturbance conditions [*Shume et al.*, 2011], and occurrence of 150 km echoes [*Rodrigues et al.*, 2013].

The present understanding of the EEF in the Brazilian sector is still quite scarce as compared with others longitude sectors. Nevertheless, significant progress is being made with the Doppler frequency of Type II echoes measured by the 50 MHz backscatter coherent radar (RESCO) set at São Luís Space Observatory (SLZ). *Denardini et al.* [2011] studied the efficiency of the penetration electric field at equatorial latitudes based on multiresolution analyzed on equatorial and interplanetary electric field. *Denardini et al.* [2013] investigate the anomalous conductivity effects on the EEF and its possible dependence of the gravity waves braking at the *E* region heights. In a more recent work, *Denardini et al.* [2015] present the dependence of the EEF with the solar activity based on the $F_{10.7}$ solar flux.

While significant studies of the electrodynamics (conductivities, electric fields, EEJ, and its plasma instability) of the *E* region have been made separately at the SLZ and JRO, comparison between these two observatories during a solar cycle has never been published. Therefore, our main motivation in this work is to study the EEJ longitudinal variations in terms of the electric field components, *Ey* and *Ez*, inferred from Doppler frequency of Type II echoes (gradient drift instability) detected with the RESCO radar and the low-power configuration of the Jicamarca radar, also known as JULIA mode (Jicamarca Unattended Long-term Studies of the Ionosphere and Atmosphere), covering the years from 2001 to 2010. The data selection yields a total of 609 days of RESCO and JULIA soundings for both systems. This work is of interest for studies of the climatology of overall ionospheric phenomenology in the equatorial and low-latitude regions, especially in the low-latitude regions due to the sparse availability of ionospheric electric field measurements.

The locations of the radars, which data are used in this study, are shown as black squares in Figure 1, and corresponding coordinates are given in Table 1. The geomagnetic equator provided by the International Geomagnetic Reference Field (IGRF-11) model [*Finlay et al.*, 2010] is shown as the dashed line for the year 2001 and the continuous line for the year 2010. The secular variation of the Earth's magnetic field drifts the geomagnetic equator away from the SLZ region leading to an apparent northwestward movement at a fixed location. The magnetic declination is around 21°W in this region. On the other hand, the geomagnetic equator changes slightly over the years in the JRO region. This peculiarity of the geomagnetic field in both regions is an additional motivation to study the variabilities of the EEF in these two longitudinal sectors. Therefore, our discussion will focus on the similarities and differences of EEF with the geomagnetic position of the radar and geomagnetic activity. The present paper is organized as follows: the basic operational parameters of the radars used in this work for observing 3 m EEJ waves are described in section 2, the methodology to infer the EEF is briefly described in section 3, the results and discussions are provided in section 4, and

Table 1. RESCO and JULIA System Specifications and Operational Parameters Used for Measurements of Doppler Frequency of Type II Echoes (Gradient Drift Instability)

Specification	RESCO (SLZ)	JULIA (JRO)
Geographic coordinates	2.33°S, 44.20°W	11.95°S, 76.87°W
Declination angle	~21°W	~4°E
Magnetic dip	~7°S	~2°N
Antenna	32 × 24 = 768 dipoles	1 × 16 = 16 Yagi elements
Data covered	From 2001 to 2009	From 2006 to 2010
Frequency	50 MHz	49.92 MHz
Height ranges	110.3 km	110.7 km
	107.7 km	107.9 km
	105.1 km	105.0 km
	102.5 km	102.2 km
Height resolution	2.6 km	954 m
Oblique beam in zenith angle	westward by 30°	westward by 23°
Peak power	40 kW (8 × 5 kW)	30 kW
Pulse width	20 μs (noncoded)	10 μs (noncoded)
Time resolution	2 min	56.32 s

our conclusions are presented in section 5. The seasonal variability and effects due to the secular variations of the magnetic equator over Brazil are presented in this issue by *Moro et al.* [2016b].

2. RESCO and JULIA Coherent Backscatter Radars

The 50 MHz RESCO radar set at SLZ is constituted basically of a coaxial collinear antenna array which consists of 32 strings of 24 dipoles (totalizing 768 dipoles) with 1/2 wavelength element separation. The array is configured so that the antenna beam can be steered electronically between the vertical and one oblique direction (±30° zenith angle) or between the two oblique directions. The westward pointed antenna beam was used in this work. The transmitter system feeds the 32 strings with ~40 kW peak power, and so they are amplified and delivered to the antenna array through duplexer-preamplifier modules. These duplexers enable transmission and reception in the same antenna array. The noncoded pulse width was set to 20 μs, and the interpulse period was set to 1 ms. Echoes between about 80 and 120 km, with a height resolution of about 2.6 km (3 km in range) and 2 min time resolution after incoherent pulse integration, arrive between the 8 and 18 local time (LT). The four ranges of radar heights around the EEJ center used in this work are centered at 102.5, 105.1, 107.7, and 110.3 km. A detailed description of the RESCO and examples of observations are given by *Abdu et al*. [2002] and *Denardini et al*. [2009, 2015].

The JULIA mode combines low-power transmitters for coherent measurements with the main Jicamarca array and has been measuring the equatorial plasma drifts at 150 km altitude since 1996 [*Hysell and Larsen*, 1997]. In recent years, a variety of configurations has been added to the JULIA mode that utilizes different antenna pointing positions and/or small sets of antennas, particularly for EEJ studies [*Chau and Hysell*, 2004]. Since interferometry data do not work effectively for electric fields measurements in the EEJ region [*Hysell et al*., 1997], we have used data collected from an antenna array of 16 widely spaced, tilted Yagi elements at JRO. The pulsing scheme for transmission is the same as for the Jicamarca main array. Echoes from 100 to 120 km arrive through a westward sidelobe with a zenith angle of 23° between 8 and 18 LT. The height resolution is about 954 m, and the time resolution is 56.32 s after incoherent pulse integration and decoding. Since the resolution of JULIA is different of the RESCO radar, we have chosen the four JULIA height ranges centered as close as possible to the RESCO height ranges. Thus, we analyze data collected at 102.2, 105.0, 107.9, and 110.7 km. The main specifications and operational parameters of the RESCO and JULIA radars, to measure the Doppler frequency of Type II echoes used in this work, are listed in Table 1.

3. Methodology

We have selected a set of 609 days of RESCO and JULIA data collected in the Brazilian and Peruvian dip equator regions, respectively. The backscatter spectra collected by both radars generally show signatures

of both Type I and Type II echoes from 8 to 18 LT. We have applied a spectral decomposition technique to every single spectrum, assuming that the experimental spectra can be decomposed in many Gaussians as stated by *Cohen* [1973] and explained in details in the recent paper by *Denardini et al.* [2015]. The Doppler frequency (f_D) of both Type I and Type II irregularities can be obtained separately.

The parameter f_D obtained from the center of frequency distribution of Type II Gaussian is converted into the Doppler velocities of Type II irregularities (V_{DII}) taking into account the radar operating frequency (f_R) and the speed of light (c) as

$$V_{DII} = \frac{c}{2f_R} f_D, \tag{1}$$

where $c/2f_R = 3$ m for the 50 MHz backscatter radars at SLZ and JRO. The resulted V_{DII} are grouped according to the height and time of data acquisition, aiming to obtain mean velocities at a given height and local time. Thus, we have the horizontal component of these mean velocities along the radar beam, which has been extensively used to determine the drift velocity of *E* region electrons (V_e) in the EEJ and for the determination of the *Ey* component [*Balsley*, 1973; *Hysell and Burcham*, 2000; *Denardini et al.*, 2013, 2015; *Moro et al.*, 2016a].

The V_{DII} velocity has contribution due to the *E* region neutral winds below ~100 km, as shown by the following expression:

$$V_{DII} = \frac{V_e}{1+\Psi_0} + \frac{V_i \Psi_0}{1+\Psi_0}, \tag{2}$$

where V_i is the ion velocity, $\Psi_0 = \nu_{in}\nu_{en}/\Omega_i\Omega_e$ is known as anisotropic factor, and ν_{in} and ν_{en} are the ion-neutral and electron-neutral collision frequencies, respectively. Electron and ion cyclotron frequencies are Ω_e and Ω_i, respectively. The anisotropic factor is comparable or larger than unity due to the high rate of ion-neutral collisions. The ion motion (essentially due to neutral wind) cannot be neglected while deriving V_e from the observed Doppler velocity below 100 km. However, above 100 km, the collision frequencies of ion-neutral and electron-neutral are significantly less, and Ψ_0 is negligibly small. Over this region, the drift velocity of the Type II irregularities represents essentially V_e [*Devasia et al.*, 2004]. Therefore, in this work we neglected the last term in equation (2) in order to derive the *Ez* component between 100 and 110 km by the relation $V_e = \mathbf{E} \times \mathbf{B}/B^2$ with a high degree of approximation, as per equation (3) [*Cohen*, 1973; *Reddy*, 1977; *Denardini et al.*, 2015]:

$$Ez = \frac{V_{DII} \quad (1+\Psi 0)B^2}{\sin(\Theta)H}, \tag{3}$$

where Θ is the zenith angle of the radar beam, B is the Earth's magnetic field flux density, and H is its horizontal component.

Physical features of the EEJ with the aid of numerical model were examined by *Richmond* [1973]. He showed that the electric field and current at a given point are strongly dependent on conditions along the entire magnetic field line. Therefore, a conductivity model [*Denardini*, 2007; *Moro et al.*, 2016a] is used to calculate the local Hall (σ_H) and Pedersen (σ_P) conductivities along the magnetic meridian overhead the radars site, i.e., SLZ and JRO, and the field line coordinates within the grid resolution of 1 km in vertical and magnetic north-south directions in order to infer *Ey* by means of equation (4):

$$Ey = \frac{\int_{-\theta}^{+\theta} \sigma_P \quad \mathbf{r}\cdot d\boldsymbol{\theta}}{\int_{-\theta}^{+\theta} \sigma_H \quad \mathbf{r}\cdot d\boldsymbol{\theta}} \cdot Ez \Rightarrow Ey = \frac{\Sigma_P}{\Sigma_H} \cdot Ez, \tag{4}$$

where $\mathbf{r}$ is the position of the magnetic field line element considering dipole geometry, θ is the magnetic latitude, $\mathbf{d}\boldsymbol{\theta}$ is the differential magnetic latitude element vector, and Σ_P and Σ_H are the field line-integrated Pedersen and Hall conductivities, respectively. The integrals presented in equation (4) are taken along the entire length of the field line between the bases of the *E* region considered in this work in the southern and northern magnetic hemispheres.

The Mass Spectrometer and Incoherent Scatter Model (NRLMSISE-00, hereafter written as MSIS) [*Picone et al.*, 2002], International Reference Ionosphere (IRI-2007) [*Bilitza and Reinisch*, 2008], and IGRF-11 empirical model outputs provide the parameters for neutral atmosphere, ionosphere, and geomagnetic field, respectively, in the magnetic field line-integrated conductivity model in order to calculate the anisotropic factor in equation

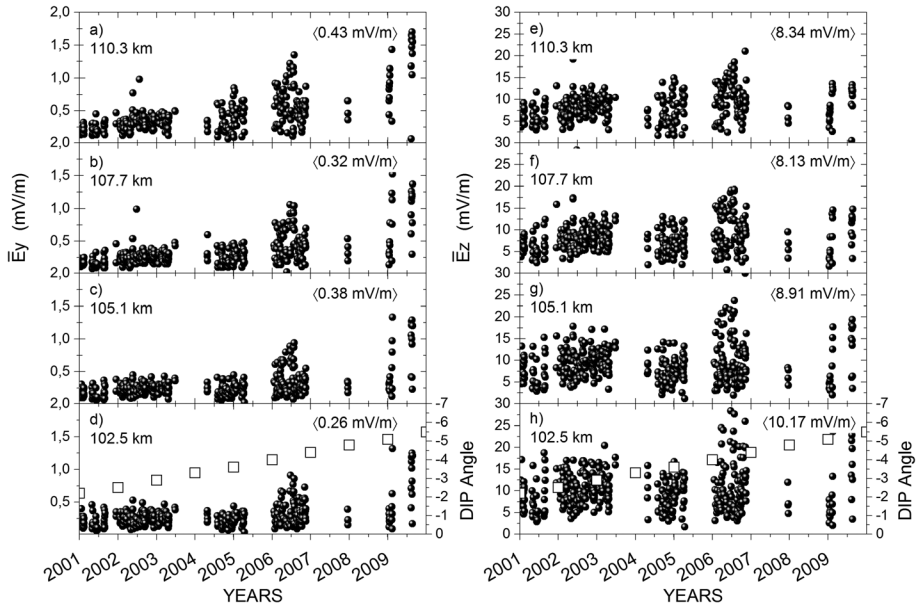

Figure 2. Daily variation of the $\overline{Ey}$ and $\overline{Ez}$ from 2001 to 2009 at the São Luís Space Observatory (SLZ), Brazil, as a function of (a–h) the height and dip equator location shown in Figures 2d and 2h.

(3) and the ionospheric conductivities in equation (4). The uncertainties in the ionospheric conductivities and the electric field components associated with these empirical model outputs were discussed recently by *Moro et al*. [2016a] in order to precisely define the confidence limit for the estimated *Ey* and *Ez* and will not be addressed here.

4. Results and Discussions

The diurnal *Ey* and *Ez* inferred from RESCO and JULIA observations at each of the four height ranges are averaged to obtain the daily mean zonal $(\overline{Ey})$ and vertical $(\overline{Ez})$ components of the EEF between 8 and 18 LT. Figure 2 shows 8 years of $\overline{Ey}$ and $\overline{Ez}$ inferred from 432 days of RESCO soundings collected from 2001 to 2009. RESCO data were not available during 2008 due to instrumental problems, and we only have 4 days of observations in 2007. A similar plot corresponding to 5 years of $\overline{Ey}$ and $\overline{Ez}$ inferred from 177 days of JULIA soundings collected from 2006 to 2010 is shown in Figure 3. In these figures, the vertical axes are set in mV/m and the years run along the horizontal axes. The graphs correspond to the four height ranges indicated in Table 1 for both observatories and identified on the top left corner of each graph. We also calculated the mean $\overline{Ey}$ (i.e., $\langle\overline{Ey}\rangle$) and mean $\overline{Ez}$ (i.e., $\langle\overline{Ez}\rangle$), shown in the top right corner of each graph, to provide an idea of the EEF strength per range height considering all soundings. In the graphs of Figures 2d, 2h, 3d, and 3h, the open squares show the estimated magnetic dip angle during the soundings in both observatories, in order to set a reference of the geomagnetic equator displacement during the period of study, in order to study the EEF with the geomagnetic position of the radar.

The mean features of the $\overline{Ey}$ and $\overline{Ez}$ at SLZ are $\overline{Ey}$ ranges from 0.04 to 1.75 mV/m between the 8 and 18 LT and $\overline{Ez}$ ranges from 1.2 to 30 mV/m. In general, we observe a positive gradient of $\langle\overline{Ey}\rangle$ with height, although $\langle\overline{Ey}\rangle$ will be more intense at 105.1 than at 107.7 km. However, we do not observe the same characteristic in $\langle\overline{Ez}\rangle$, which show negative gradient with height. Both $\overline{Ey}$ and $\overline{Ez}$ seem to have a dependency with the dip equator secular displacement effect. The geomagnetic equator drifts in a rate of ~22 min/yr (~40 km/yr); see Figure 1. Due to this drift, the geomagnetic dip angle over SLZ varied from −2.2° in 2001 to −5.1° in 2009, at 105 km.

Figure 3 shows that the $\overline{Ey}$ ranges from 0.1 to 0.69 mV/m between 8 and 18 LT at JRO, while $\overline{Ez}$ ranges from 0.78 to 23.75 mV/m. Also, we observe a positive gradient in $\langle\overline{Ey}\rangle$ with height and $\langle\overline{Ez}\rangle$, although $\langle\overline{Ez}\rangle$ will be more intense at 105 than at 107.9 km. The geomagnetic dip angle varied from −0.2° in 2006 to −0.8° in 2010, which is a very low rate (a rate of ~9 min/yr, ~16 km/year) as compared to SLZ. Another characteristic is that the EEF intensities do not vary much along the years at the JRO.

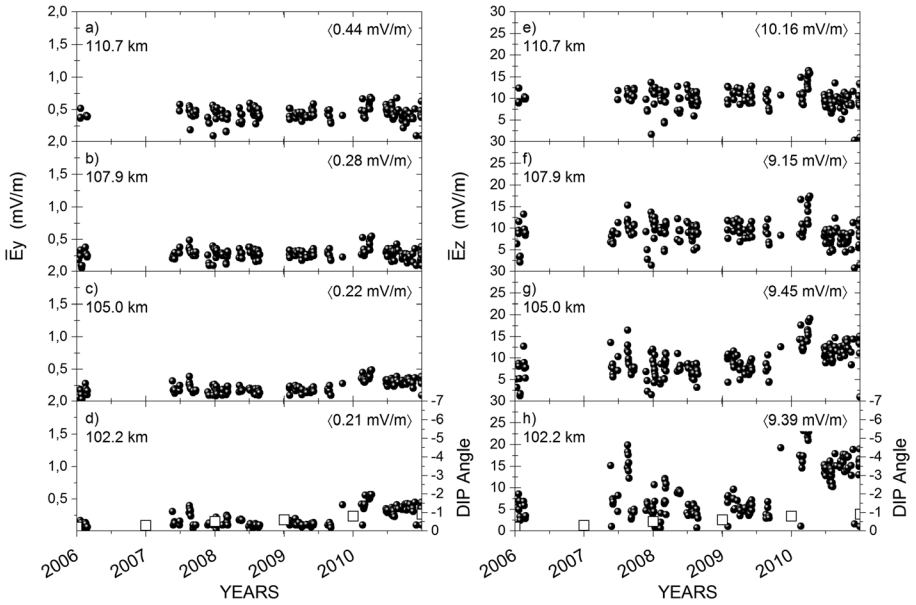

Figure 3. Daily variation of the $\overline{Ey}$ and $\overline{Ez}$ from 2006 to 2010 at the Jicamarca Radio Observatory (JRO), Peru, as a function of (a–h) the height and dip equator location shown in Figures 3d and 3h.

The similarity in the EEF at SLZ and JRO that we identify from the results of Figures 2 and 3 is that $\overline{Ey}$ and $\overline{Ez}$ are not drastically affected by the dip equator displacement along the years. This fact is clearer at SLZ since the EEFs are more intense in the year 2009. However, this was not expected since the current theories predicted that the EEJ current sheet flows along the geomagnetic dip latitudes (±3°) at 105 km altitude. The dip angle achieved this threshold in 2003 at SLZ. Nevertheless, the EEJ plasma irregularities were observed until 2009 (dip: −5.1°) once the conditions of EEJ irregularities development predicted by the linear theory [*Fejer et al*., 1975] were satisfied. Indeed, SLZ is still considered an equatorial region since the dip angle is less than 7°. JRO results corroborate with this observation in the Brazilian sector because we have observed more intense EEF in 2010 at JRO.

With respect to the differences in $\langle\overline{Ey}\rangle$ and $\langle\overline{Ez}\rangle$ at SLZ and JRO, we can list several observed characteristics. An upward gradient in $\langle\overline{Ey}\rangle$ is observed at JRO, but it is not observed in $\langle\overline{Ey}\rangle$ at SLZ. The higher values of $\langle\overline{Ey}\rangle$ are 0.43 mV/m at 110.3 km at SLZ and 0.44 mV/m at 110.7 km at JRO. The lower values of $\langle\overline{Ey}\rangle$ are found at lower altitudes in both observatories. With regard to the gradient of $\langle\overline{Ez}\rangle$, we could find a clear difference between SLZ and JRO. The higher values of $\langle\overline{Ez}\rangle$ are 10.17 mV/m at 102.5 km at SLZ and 10.16 mV/m at 110.7 km at JRO. The lower values of $\langle\overline{Ez}\rangle$ are 8.13 mV/m at 107.7 km at SLZ and 9.15 mV/m at 107.9 km at JRO.

In order to verify the behavior of the electric field components inferred from the radar data collected during the geomagnetically quiet days ($Kp \leq 3+$) only, the 432 days of RESCO soundings from 2001 to 2009 were classified and 54% were selected as acquired during geomagnetically quiet day, whereas from 177 JULIA soundings, 65% were acquired during geomagnetically quiet days. In the subsequent analysis, the electric field components inferred from the RESCO and JULIA data are averaged in order to have the mean diurnal variations of the *Ey* and *Ez* per range heights. The results are plotted in the white line in Figure 4 for SLZ and in Figure 5 for JRO. Figures 4a and 4b and 5a and 5b correspond to the mean diurnal variation of *Ey* and its mean $\langle Ey\rangle$, respectively, while the mean diurnal variation of *Ez* and its mean $\langle Ez\rangle$ are shown in Figures 4c and 4d and 5c and 5d. The error bars in Figures 4b and 4d and 5b and 5d represent the standard deviation, which is related to the Doppler velocity estimation.

The main characteristics of the EEF inferred in quiet time periods that we identify from the result shown in Figures 4 and 5 are *Ey* ranges from 0.21 to 0.35 mV/m at SLZ and from 0.23 to 0.45 mV/m at JRO. The component *Ez* ranges from 7.09 to 8.80 mV/m at SLZ and from 9.00 to 11.18 mV/m at JRO. Accordingly to our results during the quiet periods, *Ez* is at most 20–30 times *Ey* at SLZ, and *Ez* is at most 25–40 times *Ey* at JRO. The results also show that *Ey* can change only slightly in the *E* region in both longitudinal sectors.

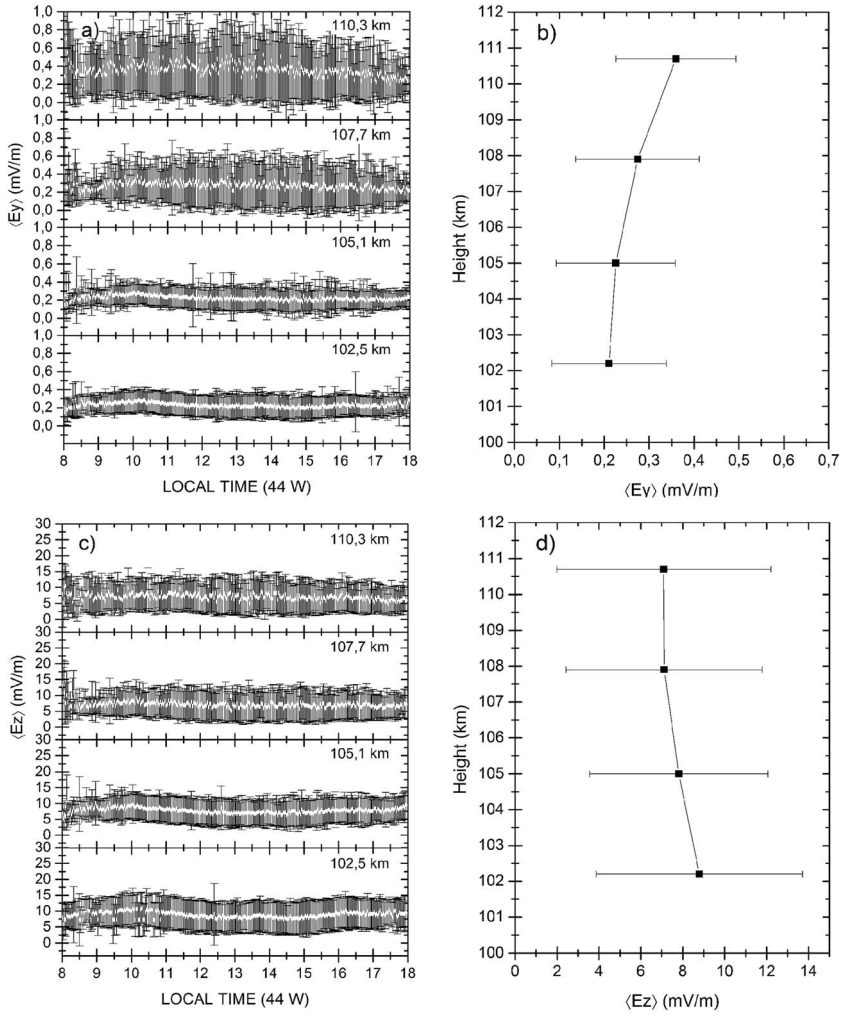

Figure 4. Diurnal variations of the (a) *Ey* and (c) *Ez* and their average (b) $< Ey >$ and (d) $< Ez >$, respectively, estimated at 102.5, 105.1, 107.7, and 110.3 km with RESCO data collected during the geomagnetically quiet days ($Kp \leq 3+$) from 2001 to 2009.

The results presented in Figures 4 and 5 clearly highlight that the *Ey* and *Ez* components vary longitudinally besides SLZ and JRO being relatively close stations, separated by just 30° of longitude. The intensity of EEF is a remarkable difference between the two longitude sectors. The EEF is stronger at JRO compared at SLZ. The maximum intensity of *Ey* is 0.45 mV/m at JRO and 0.35 mV/m at SLZ. The maximum intensity of *Ez* is 11.18 mV/m at JRO and 8.80 mV/m at SLZ. The EEF components are less intense at SLZ by about 22% as compared to that at JRO during quiet time days.

Ground-based magnetic field measurements have shown that the EEJ varies longitudinally within the South American continent between SLZ and JRO [*Shume et al*., 2010, and references therein]. The difference in *Ey* between SLZ and JRO might be caused by the difference in its modulation by atmospheric tides in the Brazilian and Peruvian sectors [*England et al*., 2006; *Vineeth et al*., 2007]. *Yamazaki et al*. [2014] reported that the irregular variability of the neutral wind produces day-to-day variations in the daily range of Sq (H) near the magnetic equator causing the daily EEJ variability. The authors have also shown that *Ey* is the main source of the day-to-day variations of EEJ. Figures 4a, 4c, 5a, and 5c also demonstrate differences in the variability of observed EEF strengths at the two stations. The degree of EEF variability is higher in the upper portion of the EEJ at SLZ. The higher EEF variability occurs in the lower portion of the EEJ at JRO. In addition, the EEFs intensify between 10 and 14 LT at JRO, which is clearer above 105 km.

The downward gradient in $\langle Ez \rangle$ shown in Figure 4d may be caused by the modeling of the anisotropic factor (equation (2)) for SLZ region. The magnetic field line-integrated conductivity model uses the MSIS-2000, IRI-

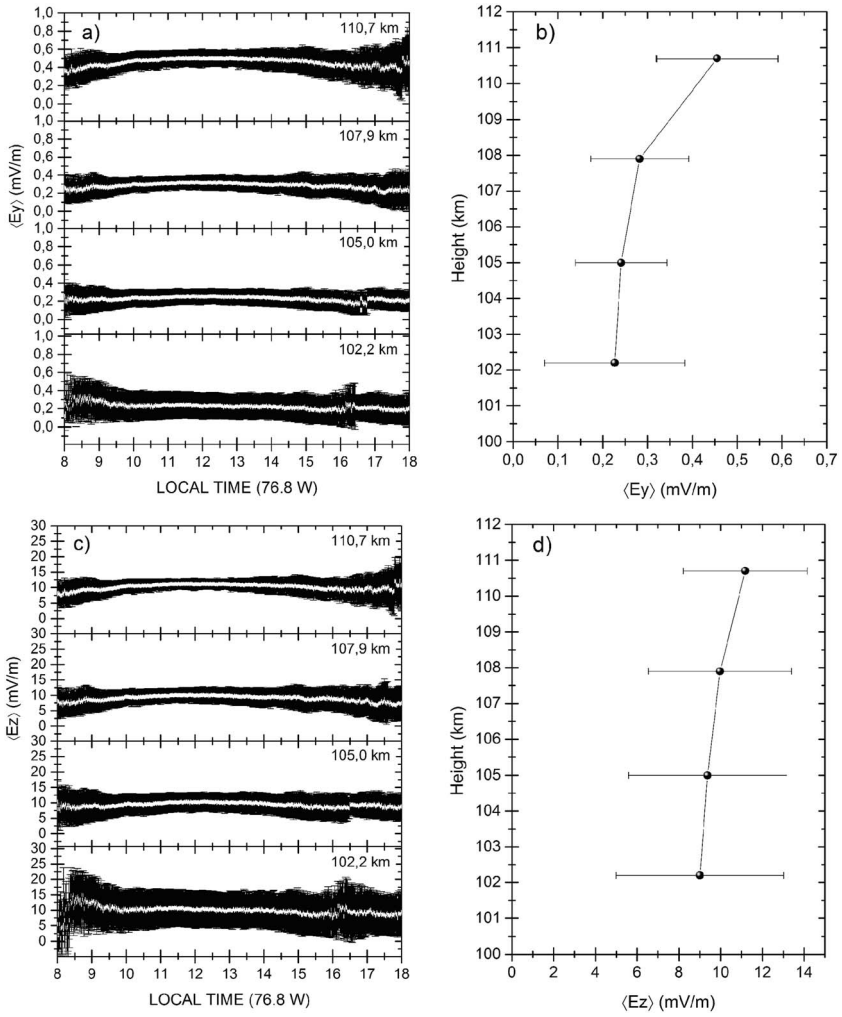

Figure 5. Diurnal variations of the (a) *Ey* and (c) *Ez* and their average (b) <*Ey*> and (d) <*Ez*>, respectively, estimated at 102.2, 105.0, 107.9, and 110.7 km with JULIA data collected during the geomagnetically quiet days ($Kp \leq 3+$) from 2006 to 2010.

2007, and IGRF-11 empirical model as input parameters for neutral atmosphere, ionosphere, and geomagnetic field, respectively. The uncertainties (or errors) in the electric fields estimate associated with these empirical model outputs for the SLZ region were studied recently by *Moro et al.* [2016a]. It is observed that the electric fields over SLZ can differ by almost 40% if the magnitude of the variables provided by the empirical models is overestimated or underestimated by 10%. One of the most significant results of the study is that the variations in the O, N_2, and O_2 densities and neutral temperature provided by the MSIS-2000 cause the largest changes in the *E* region conductivity and electric fields. In addition, the effects are higher in the lower *E* region, below ~105 km. Therefore, we could identify an upward gradient in *Ez* with height at SLZ taking into account the uncertainties in the empirical models recently discussed by *Moro et al.* [2016a].

The *Ey* component has been shown to be independent of altitude in the equatorial *F* region and closely related to the *Ey* component in the *E* region [*Woodman*, 1970; *Balsley and Woodman*, 1969]. Also, the component is responsible for the *F* region vertical drift, since it is mapped into the *F* region along electrically equipotential geomagnetic field lines. In Jicamarca sector, the *E* region electron drift velocity is about 400 m/s and an *F* region vertical velocity of about 20 m/s if *Ey* is ~0.5 mV/m [*Woodman*, 1970; *Fejer et al.*, 1979]. The east-west *F* region field and the north directed geomagnetic field produce a vertical drift of the *F* region ionization. Several works have indicated that the vertical plasma drift in the *F* region is higher in the Peruvian than in the Brazilian sector [*Fejer et al.*, 1979; *Abdu et al.*, 1981]. This fact agrees well with our EEF results, being stronger at JRO than at SLZ.

The daytime *Ey* values for quiet days presented in this work can be compared to those reported in the literature. The relationship between *Ey* and the east-west electron velocity was given for the Jicamarca location by $Ey \cong -6 \times 10^{-6} V_{DII}$ [*Balsley and Woodman*, 1971], where the electric field is expressed in V/m and the drift velocity in given in m/s. The authors reported *Ey* values in the range 0.38–2.06 mV/m using the last equation. *Balsley* [1973] also reported *Ey* values in the range 0.8–1.0 mV/m around noon for the equinoctial period during solar maximum (1967–1973). However, *Fejer et al*. [1975] pointed out that the phase velocity of the irregularities has to be multiplied by an appropriated factor, which is Ψ_0 shown in equation (2). *Reddy et al*. [1987] and *Viswanathan et al*. [1987] reported *Ey* values in the ranges 0.1–0.55 mV/m and 0.1–0.6 mV/m, respectively, taking into account the anisotropic factor. Our results from the quiet time periods indicate *Ey* values in the range 0.23–0.45 mV/m in the Peruvian sector and 0.21–0.35 mV/m in the Brazilian sector, which is in good agreement with the previews results.

The diurnal variability of *Ey* presented in the present work is less intense than the ones published by *Denardini et al*. [2013] in the Brazilian sector mainly due to two reasons: (i) the magnetic field line-integrated conductivity model was updated after their work [*Moro et al*., 2016a] and (ii) we considered here data covering the years from 2001 to 2009. The experiment ran in 2002 and 63 magnetically quiet days were selected to infer the electric fields in *Denardini et al*. [2013]. It should also be remembered that the previous solar cycle, solar cycle 23, peaked in 2000–2002 with many intense geomagnetic storms.

During geomagnetic disturbances, the EEF undergo significant deviations from their quiet day patterns due to disturbance electric field originating from the high latitude in the form of disturbance dynamo electric field and from the magnetosphere in the form of prompt penetration electric field (e.g., *Fejer* [2002] for a review). Although the data selected in the quiet time analysis are considered to be acquired in quiet days based on the *Kp* values, the auroral indices *AE* showed some disturbances (not shown here) in some days and may have produced effects in EEJ signatures in the radar returns. This point demonstrates the efficient electrodynamics coupling that exists between the auroral and equatorial current systems and will be subject of a future work. Such deviations can be clearly observed in the SLZ results when Figure 2 and Figures 4b and 4d are compared. The $\langle \overline{Ey} \rangle$ and $\langle \overline{Ez} \rangle$ shown in the top right corner of each graph in Figure 2 (all radar data set) are more intense than $< Ey >$ and $< Ez >$ values in Figure 4 (quiet data only), which may be caused by the amount of RESCO data set acquired from 2001 to 2009 during periods with $Kp > 3+$ (46% of the soundings). This is less evident in the Peruvian sector, when we compare the results in Figure 3 and Figures 5b and 5d, because the number of JULIA data set acquired from 2006 to 2010 with $Kp > 3+$ (35% of the soundings) is considerably smaller. The first observational result showing EEJ effects in the Brazilian sector due to auroral substorms even on a *Kp*-based conventional quiet day can be found in *Abdu et al*. [2003].

The discussion of the large difference in the magnetic declination angle between SLZ and JRO and its consequence in the EEF was raised in this paper, especially with the results presented in Figures 2 and 3. The separation of the geographic and dip equators being 2.33°S for São Luís and 12°S for Jicamarca may cause significant differences in the EEF seasonal variation due to the effects of neutral dynamics on EEJ instability process for the two locations. These effects will be presented on this issue by *Moro et al.* [2016b].

5. Summary and Conclusions

We have examined variabilities of the *E* region electric fields (EEF) in locations close to the magnetic equator in eastern Brazil (São Luís Space Observatory-SLZ, 2.33°S, 44.20°W) and Peru (Jicamarca Radio Observatory-JRO, 11.95°S, 76.87°W). The vertical (*Ez*) electric field component is obtained from the Doppler frequency of Type II echoes detected with RESCO and JULIA coherent backscatter radars. The eastward zonal (*Ey*) electric field component is obtained from the vertical component and the Hall-to-Pedersen ionospheric conductivity ratio. The radar soundings collected during the solar cycles 23–24 (from 2001 to 2010) are used to derive the EEF components.

The results based on more than 600 days of RESCO and JULIA soundings show that the daily mean zonal ($\overline{Ey}$) component ranges from 0.04 to 1.75 mV/m and the daily mean vertical ($\overline{Ez}$) component ranges from 1.2 to 30 mV/m between the 8 and 18 LT at SLZ. We have observed positive gradient in the mean $\overline{Ey}$, $\langle \overline{Ey} \rangle$, with height, but the same characteristic in the mean $\overline{Ez}$, $\langle \overline{Ez} \rangle$, is not observed. In the Peruvian sector, $\overline{Ey}$ ranges from 0.1 mV/m to 0.69 mV/m, while $\overline{Ez}$ ranges from 0.78 to 23.75 mV/m between 8 and 18 LT. Also, we observe a

positive gradient in $\langle\overline{Ey}\rangle$ with height. The similarity between $\overline{Ey}$ and $\overline{Ez}$ at SLZ and JRO is that they are not drastically affected by the dip equator secular displacement along the years.

The diurnal variation of *Ey* and *Ez* inferred from radar data collected during the geomagnetically quiet days ($Kp \leq 3+$) reveled that *Ey* ranges from 0.21 to 0.35 mV/m at SLZ and from 0.23 to 0.45 mV/m at JRO. The *Ez* component ranges from 7.09 mV/m to 8.80 mV/m at SLZ and from 9.00 mV/m to 11.18 mV/m at JRO, showing that the EEF varies longitudinally besides SLZ and JRO been separated by 30° of longitude. The present study shows that the *Ey* and *Ez* components are less intense in the Brazilian sector by about 22% as compared to that at the Peruvian sector.

Acknowledgments

J. Moro thanks CNPq/MCTIC (grant 312775/2015-6) and the National Space Science Center (NSSC), Chinese Academy of Sciences (CAS) for supporting his postdoctoral. C.M. Denardini thanks CNPq/MCTIC (grant 303121/2014-9) and FAPESP (grant 2012/08445-9). L.C.A. Resende thanks FAPESP (grant 2014/11198-9). S.S. Chen thanks CNPq/MCTIC (grant 312730/2015-2). The authors thank DAE/INPE for kindly providing the RESCO data. Clezio M. Denardini is responsible for the RESCO data, e-mail: clezio.denardin@inpe.br. The Jicamarca Radio Observatory is gratefully acknowledged for providing the JULIA data. The Jicamarca Radio Observatory is a facility of the Instituto Geofisico del Peru operated with support from the NSF AGS-1433968 through Cornell University (request data by e-mailing databasejro.igp.gob.pe). The authors wish to acknowledge the Editor and referees for their assistance in evaluating this paper.

References

Abdu, M. A., J. A. Bittencourt, and I. S. Batista (1981), Magnetic declination control of the equatorial F region dynamo electric field development and spread F, *J. Geophys. Res.*, *86*, 11,443–11,446, doi:10.1029/JA086iA13p11443.

Abdu, M. A., C. M. Denardini, J. H. A. Sobral, I. S. Batista, P. Muralikrishna, and E. R. de Paula (2002), Equatorial electrojet irregularities investigations using a 50 MHz back-scatter radar and a digisonde at São Luís: Some initial results, *J. Atmos. Sol. Terr. Phys.*, *64*(12–14), 1425–1434, doi:10.1016/S1364-6826(02)00106-2. [Availabe at http://www.sciencedirect.com/science/article/pii/S1364682602001062.]

Abdu, M. A., C. M. Denardini, J. H. A. Sobral, I. S. Batista, P. Muralikrishna, K. N. Iyer, O. Veliz, and E. R. de Paula (2003), Equatorial electrojet 3-M irregularity dynamics during magnetic disturbances over Brazil: Results from the new VHF radar at São Luís, *J. Atmos. Sol. Terr. Phys.*, *65*, 1293–1308, doi:10.1016/j.jastp.2003.08.011.

Aveiro, H. C., C. M. Denardini, and M. A. Abdu (2009a), Climatology of gravity waves-induced electric fields in the equatorial *E* region, *J. Geophys. Res.*, *114*, A11308, doi:10.1029/2009JA014177.

Aveiro, H. C., C. M. Denardini, and M. A. Abdu (2009b), Signatures of 2-day wave in the E-region electric fields and their relationship to winds and ionospheric currents, *Ann. Geophys.*, *27*(2), 631–638, doi:10.5194/angeo-27-631-2009.

Balsley, B. B. (1973), Electric fields in the equatorial ionosphere: A review of techniques and measurements, *J. Atmos. Terr. Phys.*, *35*, 1035–1044, doi:10.1016/0021-9169(73)90003-2.

Balsley, B. B., and R. F. Woodman (1969), On the control of the *F* region drift velocity by the *E* region electric field: Experimental evidence, *J. Atmos. Terr. Phys.*, *31*, 865–867, doi:10.1016/0021-9169(69)90167-6.

Balsley, B. B., and R. F. Woodman (1971), *Ionospheric Drift Velocity Measurements at Jicamarca, Peru (July 1967–March 1970)*, pp. 1–45 , World Data Cent. A – Upper Atmos. Geophys., Asheville, N. C.

Bilitza, D., and B. Reinisch (2008), International reference ionosphere 2007: Improvements and new parameters, *Adv. Space Res.*, *42*(4), 599–609, doi:10.1016/j.asr.2007.07.048.

Chau, J. L., and D. L. Hysell (2004), High altitude large-scale plasma waves in the equatorial electrojet at twilight, *Ann. Geophys.*, *22*, 4071–4076, doi:10.5194/angeo-22-4071-2004.

Cohen, R. (1973), Phase velocities of irregularities in the equatorial electrojet, *J. Geophys. Res.*, *78*, 2222–2231, doi:10.1029/JA078i013p02222.

Cohen, R., and K. L. Bowles (1967), Secondary irregularities in the equatorial electrojet, *J. Geophys. Res.*, *72*, 885–894, doi:10.1029/JZ072i003p00885.

Crochet, M. (1977), Radar studies of longitudinal differences in the equatorial electrojet: A review, *J. Atmos. Terr. Phys.*, *39*, 1103–1117, doi:10.1016/0021-9169(77)90019-8.

Crochet, M., C. Hanuise, and P. Broche (1979), HF radar studies of two-stream instability during an equatorial counter electrojet, *J. Geophys. Res.*, *84*, 5223–5233, doi:10.1029/JA084iA09p05223.

Denardini, C. M. (2007), A conductivity model for the Brazilian equatorial E-region: Initial results, *Braz. J. Geophys.*, *25*(2), 87–94.

Denardini, C. M., M. A. Abdu, and J. H. A. Sobral (2003), Detection of three distinct regions in the equatorial electrojet in the Brazilian sector, *Braz. J. Geophys.*, *21*(1), 65–74.

Denardini, C. M., M. A. Abdu, and J. H. A. Sobral (2004), VHF radar studies of the equatorial electrojet 3-m irregularities over Sao Luis: Day-to-day variabilities under auroral activity and quiet conditions, *J. Atmos. Sol. Terr. Phys.*, *66*(17), 1603–1613, doi:10.1016/j.jastp.2004.07.031.

Denardini, C. M., M. A. Abdu, E. R. de Paula, J. H. A. Sobral, and C. M. Wrasse (2005), Seasonal characterization of the equatorial electrojet height rise over Brazil as observed by the RESCO 50 MHz back-scatter radar, *J. Atmos. Sol. Terr. Phys.*, *67*(17–18), 1665–1673, doi:10.1016/j.jastp.2005.04.008.

Denardini, C. M., M. A. Abdu, E. R. de Paula, C. M. Wrasse, and J. H. A. Sobral (2006), VHF radar observations of the dip equatorial E-region during sunset in the Brazilian sector, *Ann. Geophys.*, *24*(6), 1617–1623, doi:10.5194/angeo-24-1617-2006.

Denardini, C. M., M. A. Abdu, H. C. Aveiro, L. C. A. Resende, P. D. S. C. Almeida, E. P. A. Olivio, J. H. A. Sobral, and C. M. Wrasse (2009), Counter electrojet features in the Brazilian sector: Simultaneous observation by radar, digital sounder and magnetometers, *Ann. Geophys.*, *27*(4), 1593–1603, doi:10.5194/angeo-27-1593-2009.

Denardini, C. M., H. C. Aveiro, P. D. S. C. Almeida, L. C. A. Resende, L. M. Guizelli, J. Moro, J. H. A. Sobral, and M. A. Abdu (2011), Daytime efficiency and characteristic time scale of interplanetary electric fields penetration to equatorial latitude ionosphere, *J. Atmos. Sol. Terr. Phys.*, *73*(11–12), 1555–1559, doi:10.1016/j.jastp.2010.09.003.

Denardini, C. M., H. C. Aveiro, J. H. A. Sobral, J. V. Bageston, L. M. Guizelli, L. C. A. Resende, and J. Moro (2013), E region electric fields at the dip equator and anomalous conductivity effects, *Adv. Space Res.*, *51*(10), 1857–1869, doi:10.1016/j.asr.2012.06.003.

Denardini, C. M., J. Moro, L. C. A. Resende, S. S. Chen, N. J. Schuch, and J. E. R. Costa (2015), E region electric field dependence of the solar activity, *J. Geophys. Res. Space Physics*, *120*, 8934–8941, doi:10.1002/2015JA021714.

de Paula, E. R., and D. L. Hysell (2004), The São Luís 30 MHz coherent scatter ionospheric radar: System description and initial results, *Radio Sci.*, *39*, RS1014, doi:10.1029/2003RS002914.

Devasia, C. V., N. Jyoti, K. S. V. Subbarao, D. Tiwari, C. R. Reddi, and R. Sridharan (2004), On the role of vertical electron density gradients in the generation of type II irregularities associated with blanketing ES (ESb) during counter equatorial electrojet events: A case study, *Radio Sci.*, *39*, RS3007, doi:10.1029/2002RS002725.

England, S. L., S. Maus, T. J. Immel, and S. B. Mende (2006), Longitudinal variation of the E-region electric fields caused by atmospheric tides, *Geophys. Res. Lett.*, *33*, L21105, doi:10.1029/2006GL027465.

Farley, D. T. (1985), Theory of equatorial electrojet plasma waves: New developments and current status, *J. Atmos. Terr. Phys.*, *47*, 729–744, doi:10.1016/0021-9169(85)90050-9.
Farley, D. T., and B. B. Balsley (1973), Instabilities in the equatorial electrojet, *J. Geophys. Res.*, *78*, 227–239, doi:10.1029/JA078i001p00227.
Farley, D. T., B. G. Fejer, and B. B. Balsley (1978), Radar observations of two-dimensional turbulence in the equatorial electrojet: 3. Nighttime observations of type I waves, *J. Geophys. Res.*, *83*, 5625–5632, doi:10.1029/JA083iA12p05625.
Fejer, B. G. (2002), Low latitude storm time ionospheric electrodynamics, *J. Atmos. Sol. Terr. Phys.*, *64*, 1401–1408, doi:10.1016/S1364-6826(02)00103-7.
Fejer, B. G., D. T. Farley, B. B. Balsley, and R. F. Woodman (1975), Vertical structure of the VHF backscattering region in the equatorial electrojet and the gradient drift instability, *J. Geophys. Res.*, *80*, 1313–1324, doi:10.1029/JA080i010p01313.
Fejer, B. G., D. T. Farley, R. F. Woodman, and C. Calderon (1979), Dependence of equatorial *F* region vertical drifts on seasonal and solar cycle, *J. Geophys. Res.*, *84*, 5792–5796, doi:10.1029/JA084iA10p05792.
Finlay, C. C., et al. (2010), International geomagnetic reference field: The eleventh generation, *Geophys. J. Int.*, *183*, 1216–1230, doi:10.1111/j.1365-246X.2010.04804.x.
Forbes, J. M. (1981), The equatorial electrojet, *Rev. Geophys.*, *19*, 469–504, doi:10.1029/RG019i003p00469.
Hysell, D. L., and J. D. Burcham (2000), Ionospheric electric field estimates from radar observations of the equatorial electrojet, *J. Geophys. Res.*, *105*, 2443–2460, doi:10.1029/1999JA900461.
Hysell, D. L., and M. F. Larsen (1997), JULIA radar studies of electric fields in the equatorial electrojet, *Geophys. Res. Lett.*, *24*(13), 1687–1690.
Kudeki, E., and F. Sürücü (1991), Radar interferometric imaging of field-aligned plasma irregularities in the equatorial electrojet, *Geophys. Res. Lett.*, *18*, 41–44, doi:10.1029/90GL02603.
Moro, J. M., C. M. Denardini, L. C. A. Resende, S. S. Chen, and N. J. Schuch (2016a), Influence of uncertainties of the empirical models for inferring the E-region electric fields at the dip equator, *Earth Planets Space*, doi:10.1186/s40623-016-0479-0.
Moro, J. M., C. M. Denardini, L. C. A. Resende, S. S. Chen, and N. J. Schuch (2016b), Equatorial E-region electric fields at the dip equator: 2. Seasonal variabilities and effects over Brazil due to the secular variation of the magnetic equator, *J. Geophys. Res. Space Physics*, doi:10.1002/2016JA022753.
Patra, A. K., D. Tiwari, C. V. Devasia, T. K. Pant, and R. Sridharan (2005), East-west asymmetries of the equatorial electrojet 8.3 m type-2 echoes observed over Trivandrum and a possible explanation, *J. Geophys. Res.*, *110*, A11305, doi:10.1029/2005JA011124.
Picone, J. M., A. E. Hedin, D. P. Drob, and A. C. Aikin (2002), NRLMSISE-00 empirical model of the atmosphere: Statistical comparisons and scientific issues, *J. Geophys. Res.*, *107*(A12), 1468, doi:10.1029/2002JA009430.
Reddy, C. A. (1977), The equatorial electrojet and the associated plasma instabilities, *J. Sci. Ind. Res.*, *36*, 580–589.
Reddy, C. A., and C. V. Devasia (1976), Short-period fluctuations of equatorial electrojet, *Nature*, *261*(5559), 396–397, doi:10.1038/261396a0.
Reddy, C. A., V. V. Somayajulu, and K. S. Viswanathan (1981), Backscatter radar measurements of storm-time electric field changes in the equatorial electrojet, *J. Atmos. Terr. Phys.*, *43*, 817–827, doi:10.1016/0021-9169(81)90059-3.
Reddy, C. A., B. T. Vikramkumar, and K. S. Viswanathan (1987), Electric fields and currents in the equatorial electrojet deduced from VHF radar observations—I. A method of estimating electric fields, *J. Atmos. Terr. Phys.*, *49*, 183–191, doi:10.1016/0021-9169(87)90053-5.
Richmond, A. D. (1973), Equatorial electrojet—I. Development of a model including winds and instabilities, *J. Atmos. Terr. Phys.*, *35*, 1083–1103, doi:10.1016/0021-9169(73)90007-X.
Rodrigues, F. S., E. B. Shume, E. R. de Paula, and M. Milla (2013), Equatorial 150 km echoes and daytime F region vertical plasma drifts in the Brazilian longitude sector, *Ann. Geophys.*, *31*, 1867–1876, doi:10.5194/angeo-31-1867-2013.
Shume, E. B., C. M. Denardini, E. R. de Paula, and N. B. Trivedi (2010), Variabilities of the equatorial electrojet in Brazil and Perú, *J. Geophys. Res.*, *115*, A06306, doi:10.1029/2009JA014984.
Shume, E. B., E. R. de Paula, and M. A. Abdu (2011), Modulation of equatorial electrojet plasma waves by overshielding electric field during geomagnetic storms, *J. Geophys. Res.*, *116*, A08302, doi:10.1029/2010JA016353.
Vineeth, C., T. K. Pant, C. V. Devasia, and R. Sridharan (2007), Atmosphere: Ionosphere coupling observed over the dip equatorial MLTI region through the quasi 16 day wave, *Geophys. Res. Lett.*, *34*, L12102, doi:10.1029/2007GL030010.
Viswanathan, K. S., B. T. Vikramkumar, and C. A. Reddy (1987), Electric fields and currents in the equatorial electrojet deduced from VHF radar observations—II. Characteristics of electric fields on quiet and disturbed days, *J. Atmos. Terr. Phys.*, *49*, 193–200, doi:10.1016/0021-9169(87)90054-7.
Viswanathan, K. S., R. B. Nair, and P. B. Rao (1993), Simultaneous observations of *E* and *F* region electric field fluctuations at the magnetic equator, *J. Atmos. Terr. Phys.*, *55*, 185–192, doi:10.1016/0021-9169(93)90123-G.
Woodman, R. F. (1970), Vertical drifts velocities and east-west electric fields at the magnetic equator, *J. Geophys. Res.*, *75*, 6249–6259, doi:10.1029/JA075i031p06249.
Woodman, R. F., and J. L. Chau (2002), First Jicamarca radar observations of two-stream *E region* irregularities under daytime counter electrojet conditions, *J. Geophys. Res.*, *107*(A12), 1482, doi:10.1029/2002JA009362.
Yamazaki, Y., A. D. Richmond, A. Maute, H.-L. Liu, N. Pedatella, and F. Sassi (2014), On the day-to-day variation of the equatorial electrojet during quiet periods, *J. Geophys. Res. Space Physics*, *119*, 6966–6980, doi:10.1002/2014JA020243.

Erratum

The Acknowledgment statement in the originally published article was incomplete. This version contains all necessary acknowledgments and may be considered the final version of record.